Journal of Controlled Release 266 (2017) 287–300

Contents lists available at ScienceDirect

Journal of Controlled Release

journal homepage: www.elsevier.com/locate/jconrel

Co-delivery of nucleoside-modified mRNA and TLR agonists for cancer immunotherapy: Restoring the immunogenicity of immunosilent mRNA

Rein Verbeke[a,b], Ine Lentacker[a,b], Laura Wayteck[a,b], Karine Breckpot[c], Mieke Van Bockstal[d], Benedicte Descamps[e], Christian Vanhove[e], Stefaan C. De Smedt[a,b,*,1], Heleen Dewitte[a,b,c,1]

[a] Ghent Research Group on Nanomedicines, Faculty of Pharmacy, Ghent University, Ottergemsesteenweg 460, 9000 Ghent, Belgium
[b] Cancer Research Institute Ghent (CRIG), Ghent University Hospital, De Pintelaan 185, 9000 Ghent, Belgium
[c] Laboratory for Molecular and Cellular Therapy, Department of Biomedical Sciences, Medical School of the Vrije Universiteit Brussel (VUB), Laarbeeklaan 103, 1050 Jette, Belgium
[d] Department of Pathology, Ghent University Hospital, De Pintelaan 18, 9000 Ghent, Belgium
[e] Infinity Lab, Institute Biomedical Technology, Medical Imaging and Signal Processing, Ghent University, De Pintelaan 185, 9000 Ghent, Belgium

ARTICLE INFO

Keywords:
mRNA vaccination
MPLA
Adjuvant
Type I interferon
Lipid nanoparticle
Dendritic cell

Chemical compounds studied in this article:
DOTAP (PubChem CID: 6437371)
DOPE (PubChem CID: 9546757)
Cholesterol (PubChem CID: 5997)
MPLA (PubChem CID: 5043498)
CFSE (PubChem CID: 16211581)
SIINFEKL (PubChem CID: 71311993)
Pseudouridine (PubChem CID: 57369533)
5-Methylcytidine (PubChem CID: 92918)

ABSTRACT

This study reports on the design of mRNA and adjuvant-loaded lipid nanoparticles for therapeutic cancer vaccination. The use of nucleoside-modified mRNA has previously been shown to improve the translational capacity and safety of mRNA-therapeutics, as it prevents the induction of type I interferons (IFNs). However, type I IFNs were identified as the key molecules that trigger the activation of antigen presenting cells, and as such drive T cell immunity. We demonstrate that nucleoside-modified mRNA can be co-delivered with the clinically approved TLR agonist monophosphoryl lipid A (MPLA). As such, we simultaneously allow high antigen expression *in vivo* while substituting the type I IFN response by a more controllable adjuvant. This strategy shows promise to induce effective antigen-specific T cell immunity and may be useful to enhance the safety of mRNA vaccines.

1. Introduction

Increasing knowledge on the interplay between the immune system and tumors has encouraged cancer researchers and oncologists to develop strategies which exploit immune cells in the battle against cancer. Cancerous cells undergo genetic and epigenetic changes, each of which can advance the tumor cell growth. At the same time they can lead to abnormal protein production and generate proteins expressed exclusively on tumor cells. These tumor antigens (TAs), called tumor specific antigens, provide the immune system with the anchor points to interact with the tumor cells. More specifically, cytotoxic T lymphocytes ($CD8^+$ T cells) have been pinpointed as the key effector cells in cancer immunotherapy since they have the capacity to selectively recognize and kill tumor cells [1,2]. Unfortunately, despite the expression of TAs, tumor cells may often not be seen as a threat by the immune system as they strongly resemble normal cells and do not provide suitable danger signals. In addition, the immune system will often spare the poorly immunogenic tumor cells, allowing them to outgrow from the heterogeneous tumor tissue and to create an immunosuppressive tumor microenvironment [3,4].

Dendritic cells (DCs), as potent antigen presenting cells (APCs), play a crucial role in the initiation and regulation of adaptive immune responses and are ideal target cell types to (re)awaken the immune system. To activate T cell-mediated immunity against cancer, it is crucial that TAs are delivered to these DCs, together with inflammatory or danger stimuli. As such, DCs can be modified to (a) present TA epitopes complexed with major histocompatibility complex (MHC) molecules on their surfaces and (b) exhibit an activated phenotype,

* Corresponding author at: Laboratory for General Biochemistry and Physical Pharmacy, Ottergemsesteenweg 460, 9000 Ghent, Belgium.
E-mail address: Stefaan.DeSmedt@UGent.be (S.C. De Smedt).
[1] Last authors contributed equally to this work.

http://dx.doi.org/10.1016/j.jconrel.2017.09.041
Received 1 June 2017; Received in revised form 21 September 2017; Accepted 29 September 2017
Available online 05 October 2017

with the expression of co-stimulatory molecules and production of inflammatory cytokines, providing the necessary T cell stimulatory signals.

In vitro transcribed (IVT) mRNA encoding full-length TAs or selected antigenic epitopes is a well-suited platform to manufacture personalized cancer vaccines with GMP quality [5]. In mRNA-based strategies, DCs are loaded with genetic information for the transient expression of (multiple) selected TAs. Hence the antigenic proteins will accumulate inside the DC's cytoplasm, resulting in preferential association with MHC class I molecules and therefore presentation to $CD8^+$ T cells. mRNA as an active pharmaceutical ingredient in cancer immunotherapy has been validated using an *ex vivo* approach, where isolated DCs are activated and loaded with TA-mRNA, after which the cells are re-injected into the patient as a cellular vaccine [6,7].

Nowadays, there is a growing interest in finding ways to deliver mRNA to DCs *in vivo*[8,9]. This could not only circumvent the laborious and patient-specific *ex vivo* DC culture and manipulation, it also holds promise in targeting multiple immune players (*e.g.* several DC subsets, macrophages, B cells) in their natural habitat (*e.g.* tumor tissue, skin, lymph nodes, and spleen), as such engineering the local environment for cancer vaccination [10–12]. Unfortunately, mRNAs are rapidly degraded by nucleases *in vivo* and therefore only locally applicable (*e.g.* intranodal, -dermal or -muscular injections) [13–15]. In this context, lipid-based nanoparticles, also referred to as mRNA lipoplexes, seem promising as they can package the mRNA to protect it against degradation while aiding the transport and delivery of mRNA into cells *in vivo*[12,16–19]. For this, they need to remain stable in blood and be able to be taken up by APCs. Subsequently, the mRNA lipoplexes must cross the (intra)cellular barriers to deliver the mRNA inside the cytosol and induce sufficient antigen expression levels to ensure “the antigen presentation signal”.

In addition, to prime the proliferation of potent $CD8^+$ T cells the mRNA lipoplexes must provide adequate immune stimuli and mediate the DC activation (*i.e.* “the activation signal”). It has previously been shown that the delivery of mRNA induces innate immune responses by binding to danger-sensing receptors, including endosomal Toll like receptors (TLRs, TLR7, TLR8 and TLR3) and cytosolic RNA sensors (*e.g.* RIG-I and MDA-5) [20–23]. As such, the intracellular mRNA immune recognition triggers an antiviral DC activation state, which is especially marked by a strong release of type I interferons (IFNs).

Recently, experiments with distinct mRNA lipoplex formulations, administered *via* various routes, identified this type I IFN production as the main driver for effective T cell activation and anticancer immunity [19,24,25]. However, a number of other studies have debated this beneficial role of type I IFNs in mRNA vaccination [26–29]. Indeed, type I IFN initiates an antiviral-like response to defend the host cells against foreign nucleic acids. We and others have shown that this can strongly reduce the mRNA intracellular stability and translation, which can affect the vaccine effectiveness [27,29–31]. In addition, the strong induction of type I IFNs may also raise some important safety concerns.

To improve mRNA stability and translation capacity, naturally occurring modified nucleotides can be incorporated into the mRNA transcript, such as pseudouridine (Ψ), N^1-methylpseudouridine (m1Ψ) and 5-methylcytidine (5meC) [32–36]. By using nucleoside-modified mRNA, the intracellular mRNA recognition by TLR3, TLR7, and TLR8 can be reduced, which makes the mRNA ‘immunosilent’ and avoids the release of type I IFNs. Furthermore, nucleotide modifications can render the RNA more resistant to enzymatic degradation. Of course, this comes together with a loss of RNA's self-adjuvant-effect, affecting hence DC activation and T-cell priming. In this study we investigate whether the simultaneous delivery of nucleoside-modified mRNA and the TLR4 agonist monophosphoryl lipid A (MPLA), may ensure both a high antigen expression as well as a strong immune activation. Prior research has shown that hydration of lipids and MPLA spontaneously self-assemble into the form of liposomes, resulting in adjuvant systems which show adequate clinical potency and safety for vaccination purposes [37–39]. As such, we designed a lipid nanoparticle in which both nucleoside-modified mRNA and MPLA can be encapsulated. Our results show that the reduced DC activation when nucleoside-modified mRNA (5meC, Ψ) is used, can be compensated by embedding MPLA in the lipid bilayer of the lipoplexes, hence achieving a high capacity to induce T cell immunity without the strong induction of type I IFNs. As such, we show for the first time the attractive approach of combining nucleoside-modified mRNA with a TLR agonist.

2. Results

2.1. Physicochemical characterization and stability of mRNA lipoplexes in serum

We initially evaluated mRNA lipoplexes with a different lipid composition. The mRNA lipoplexes were composed of the cationic lipid DOTAP (1,2-dioleoyloxy-3-trimethylammonium propane chloride) and a helper lipid, either DOPE (1,2-dioleoyl-sn-glycero-3-phosphoethanolamine) or cholesterol. Interestingly, we found that DOTAP-cholesterol mRNA lipoplexes were superior in transfecting murine bone marrow-derived (BM)-DCs over the widely reported DOTAP-DOPE mRNA lipoplexes. Fig. 1 shows that when the transfection was performed in serum-containing culture medium, DOTAP-DOPE mRNA lipoplexes (nearly) failed in transfecting (BM)-DCs while DOTAP-cholesterol

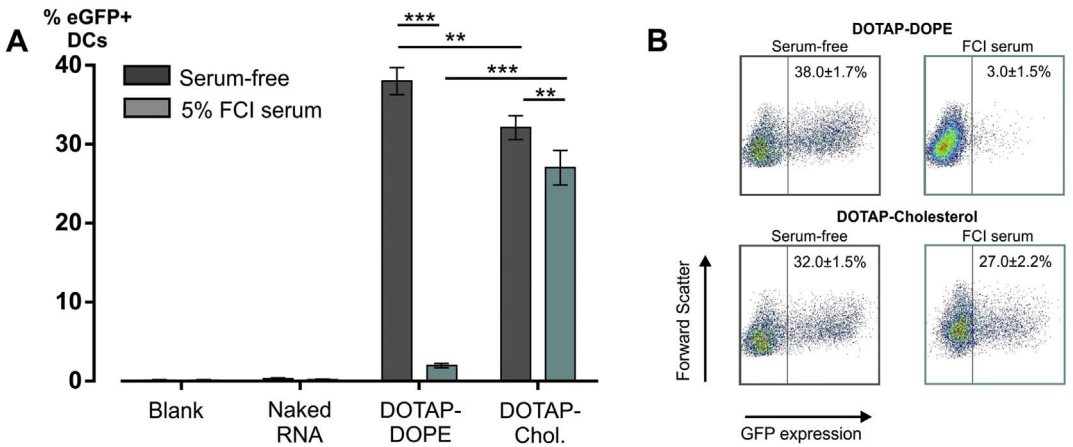

Fig. 1. Transfection efficiency of DOTAP-cholesterol *versus* DOTAP-DOPE mRNA lipoplexes. (A) Percentage of enhanced green fluorescent protein (eGFP) transfected BM-DCs 24 h after the cells were incubated with DOTAP-DOPE/mRNA or DOTAP-cholesterol/mRNA lipoplexes (using unmodified mRNA). Transfections were performed in serum-free medium (OptiMem®) and serum-containing medium. (B) Representative flow cytometry scatter plots of transfected DCs. DCs were gated based on CD11c surface staining.

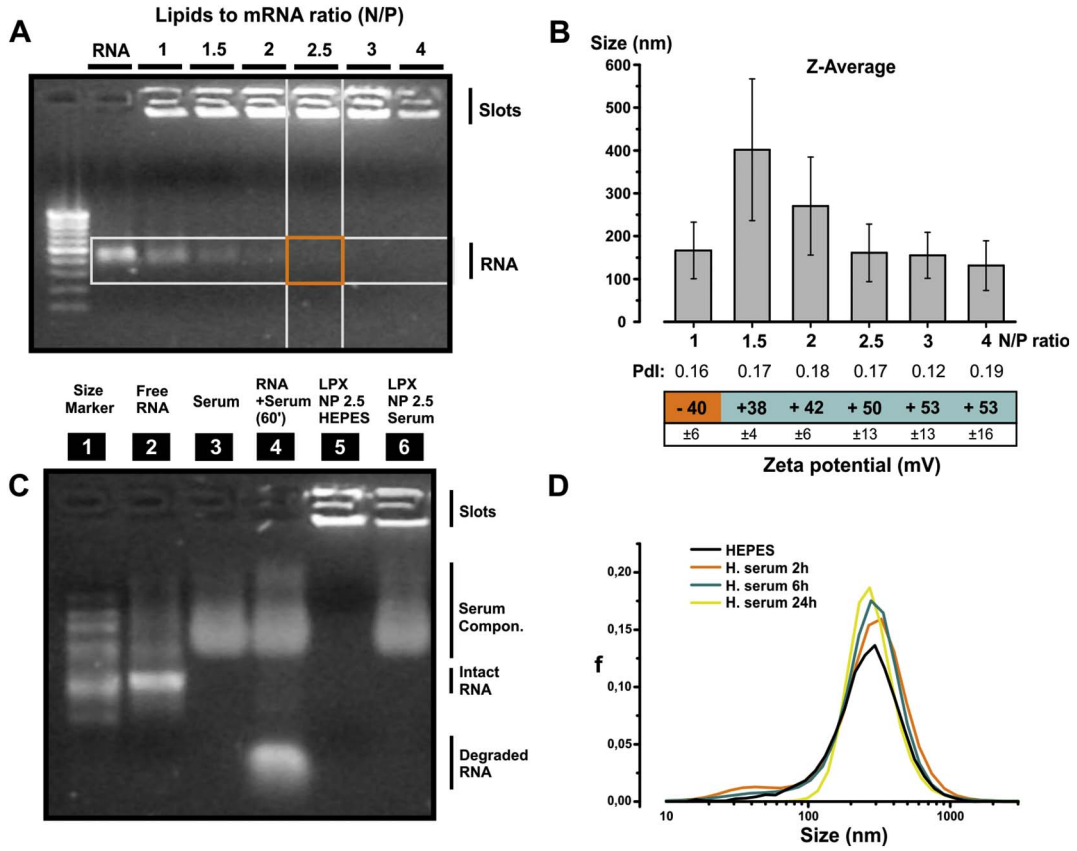

Fig. 2. Characterization of mRNA lipoplexes in serum conditions. (A) Gel electrophoresis on "naked" mRNA and DOTAP-cholesterol/mRNA lipoplexes at different N/P ratios demonstrates complete mRNA complexation at the N/P ratio of 2.5; note that unmodified mRNA was used. A molecular weight marker with bands at a range of 0.25 to 10 kb was included to provide size determination of the RNA (B) Size (Z average), polydispersity index (PdI) and zeta potential of mRNA lipoplexes (dose of 1 μg mRNA) dispersed in HEPES buffer at increasing N/P ratios. (C) Integrity of the mRNA lipoplexes in human serum, determined by gel electrophoresis: "naked" mRNA in RNase free water (lane 2), 50% human serum without mRNA (lane 3), "naked" mRNA after 1 h in 50% human serum at 37 °C (lane 4), mRNA lipoplexes after 2 h in HEPES buffer at 37 °C (lane 5), and mRNA lipoplexes after 2 h in 50% human serum at 37 °C (lane 6), and (D) Size analysis (by fSPT) on mRNA lipoplexes (Cy5-labelled mRNA) dispersed in HEPES buffer, or incubated in human serum at 37 °C for 2 h, 6 h and 24 h.

mRNA lipoplexes were successful, making them better suited for *in vivo* use. Therefore, in our further experiments we evaluated DOTAP-cholesterol liposomes carrying either (a) unmodified mRNA, (b) nucleoside-modified mRNA (5meC, Ψ), or (c) nucleoside-modified mRNA combined with the adjuvant MPLA.

Subsequently we focused on the behavior of DOTAP-cholesterol mRNA lipoplexes in serum (*in vitro*) in more detail. To assure complete mRNA complexation and as such protection of mRNA against enzymatic degradation, we investigated mRNA lipoplexes with a varying N/P ratio (*i.e.* 'charge ratio'). From the gel electrophoresis experiments on DOTAP-cholesterol/mRNA lipoplexes (using unmodified mRNA; Fig. 2A) it can be concluded that complete complexation of the mRNA occurred starting from an N/P ratio of 2.5. Hence N/P 2.5 mRNA lipoplexes were selected for further experiments. At this charge ratio, the lipoplexes had a mean size of 160 nm and a zeta potential of + 50 mV (Fig. 2B). Keeping the same N/P ratio, but using nucleoside-modified mRNA (instead of unmodified mRNA) did not change the physicochemical properties of the complexes. Also, when mRNA was complexed with liposomes containing 0.5 mol% MPLA, the physicochemical properties of the mRNA lipoplexes remained the same (Supplementary Fig. S1).

To predict the stability of the mRNA lipoplexes *in vivo* and to avoid pre-mature release of the mRNA upon parental injection of the complexes, we incubated the mRNA lipoplexes in human serum for 2 h at 37 °C. As shown in the gel electrophoresis experiment (Fig. 2C), lipoplexes carrying (unmodified) mRNA did not dissociate after incubation in 50% serum, providing adequate protection of the mRNA against degradation. Similar observations were made when lipoplexes were incubated in enzyme solution of RNase (Supplementary Fig. S2). Subsequently we measured the extent of mRNA lipoplex aggregation in serum with fluorescence single particle tracking (fSPT). Fig. 2D clearly demonstrates that the mRNA lipoplexes retain their initial size and do not aggregate in serum-containing medium. Interestingly, this indicates that the inclusion of a PEGylated lipid, typically used to prevent aggregation of lipoplexes, is redundant in this liposomal formulation.

2.2. *In vitro* mRNA transfection and activation of DCs by DOTAP-cholesterol/mRNA lipoplexes

The capacity of the mRNA lipoplexes to (a) transfect DCs and (b) subsequently induce the DC activation was first evaluated in an *in vitro* BM-DC model. These experiments were performed in an *in vivo*-mimicking (serum-containing) setting to ease the *in vitro*-to-*in vivo* translation.

To assess the transfection capacity of the mRNA lipoplexes, BM-DCs were incubated with firefly luciferase (fLuc) mRNA lipoplexes and luciferase activity was measured after 6 h. As shown in Fig. 3A, the use of nucleoside-modified mRNA (5meC, Ψ) increased the fLuc levels up to 2 orders of magnitude. Interestingly, the co-delivery of modified mRNA with the adjuvant MPLA resulted in the highest transfection, although it was previously reported that TLR agonists and DC maturation could limit the internalization of mRNA, thereby reducing the overall expression [40,41]. In addition, BM-DCs were transfected with lipoplexes containing nucleoside-modified mRNA encoding eGFP, and 24 h later analyzed by flow cytometry (Fig. 3B). Nucleoside-modified mRNA lipoplexes achieved a transfection efficiency of approximately 40%.

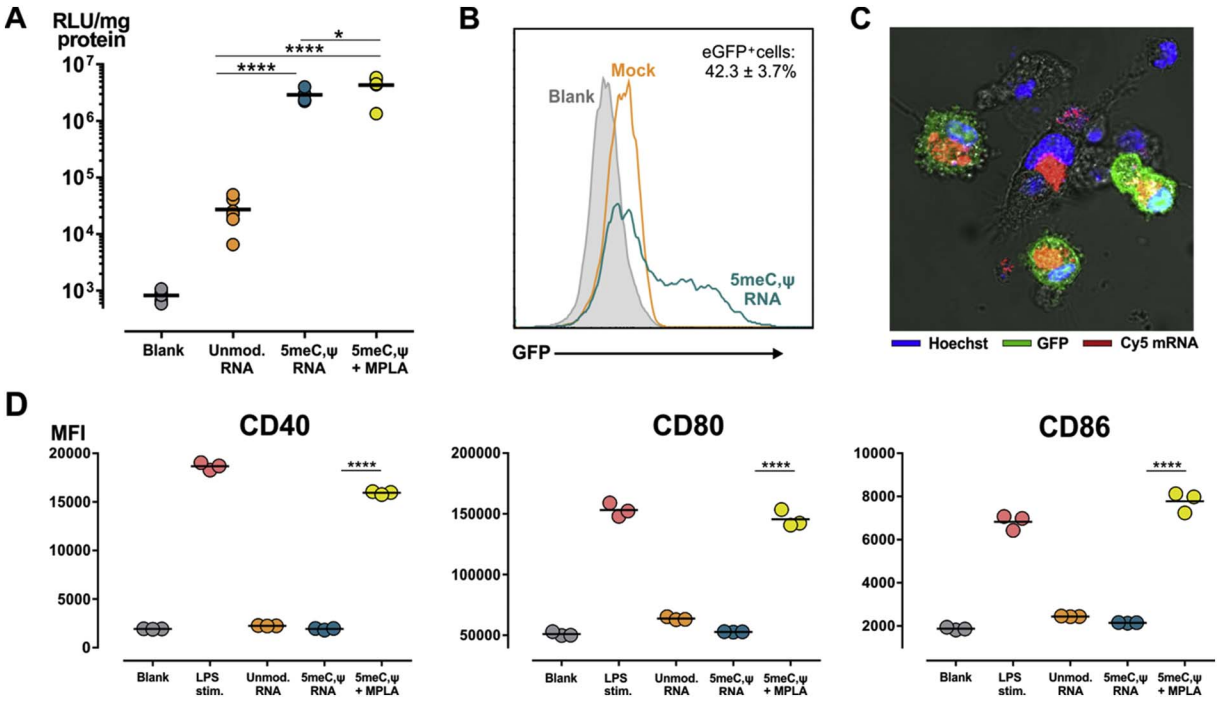

Fig. 3. *In vitro* evaluation of mRNA lipoplexes on BM-DCs. The transfection efficiency was measured 6 h after the addition of the mRNA lipoplexes to the cells. (A) fLuc activity (expressed in relative light units (RLU) per mg protein) of BM-DCs transfected with three different mRNA lipoplexes containing respectively unmodified-, nucleoside-modified (5meC, Ψ)- or nucleoside-modified fLuc mRNA and MPLA (5meC, Ψ + MPLA) ($n = 6$). (B) Representative histograms of BM-DCs transfected with nucleoside-modified (5meC, Ψ) eGFP mRNA compared to mock-transfected (OVA encoding mRNA, 5meC, Ψ) and untreated cells (blank) ($n = 5$). (C) Representative confocal image of the cellular uptake and eGFP transfection of Hoechst-stained BM-DCs (blue) transfected with lipoplexes containing GFP-encoding (green), Cy5 labelled (red) nucleoside-modified mRNA. (D) DC activation was evaluated 24 h after transfection. Untreated DCs (blank), LPS-stimulated DCs (positive control) and DCs incubated with the different mRNA lipoplexes were analyzed for the expression of the activation markers CD40, CD80 and CD86. The graph depicts the mean fluorescence intensity (MFI) of the expression of the activation markers on the surface of the BM-DCs after transfection with the different mRNA lipoplexes ($n = 3$). (For interpretation of the references to colour in this figure legend, the reader is referred to the web version of this article.)

Fig. 3C shows the transfection of BM-DCs with lipoplexes carrying nucleoside-modified mRNA encoding eGFP labelled with Cy5-dye. The Cy5 fluorescence allows visualizing the cellular uptake of the mRNA lipoplexes, while the eGFP signal requires endosomal escape of mRNA to the cytosol and translation into a functional protein. Although all of the cells seem to have taken up mRNA lipoplexes, only a smaller percentage of BM-DCs showed detectable expression of eGFP, which indicates that the endosomal/lysosomal pathway remains a major barrier for mRNA expression.

Subsequently we evaluated to what extent the mRNA lipoplexes were able to activate BM-DCs. As shown in Fig. 3D, when BM-DCs were incubated for 24 h with lipoplexes complexing either unmodified- or nucleoside-modified mRNA, we could not detect any relevant changes in the expression levels of the activation markers CD40, CD80 and CD86. Furthermore, we could not measure relevant cytokine levels of IL-12p70, IL-10 or IFN-α in the mRNA transfected DC cultures (Supplementary Fig. S3). These results suggest that BM-DCs lack responsiveness to the "self-adjuvant" effect of mRNA. In contrast, when BM-DCs were incubated with MPLA containing mRNA lipoplexes, which is a potent activator of the cell surface receptor TLR4, they matured to a similar extent as BM-DCs treated with lipopolysaccharide (LPS). Overall, these experiments emphasize that molecular adjuvants, such as MPLA, can be used to improve the mRNA lipoplexes' capacity to activate DCs and, importantly, without affecting their transfection efficiency.

2.3. Biodistribution, mRNA delivery efficiency and cellular uptake of mRNA lipoplexes after intravenous administration

2.3.1. Biodistribution and in vivo transfection efficiency of mRNA lipoplexes

In a first set of *in vivo* experiments, we simultaneously evaluated the biodistribution and *in vivo* transfection efficiency of the lipoplex formulations after systemic administration in C57BL/6 mice. To be able to track the localization of the mRNA lipoplexes *in vivo*, 1 mol% of the lipophilic dye DiR was included in the cationic liposome formulation before mRNA complexation. Additionally, we used fLuc mRNA as a reporter gene to evaluate mRNA expression *in vivo*. Mice were injected intravenously *via* the tail vein at a dose of 10 μg mRNA and 5–6 h later, the biodistribution and *in vivo* transfection efficiency of the mRNA lipoplexes were simultaneously evaluated.

Fig. 4A and B show representative whole body images of the injected mice. All three mRNA lipoplex formulations had a very similar biodistribution: mRNA lipoplexes mainly accumulated in the lungs, spleen and liver. Moreover, we could also detect mRNA lipoplexes in the bone marrow of the hind legs and at the injection site. No signal was detected in the heart, kidneys and intestines (see Supplementary Fig. S4). To quantify the accumulation of the mRNA lipoplexes in specific organs, lungs, spleen and liver were isolated and imaged *ex vivo*. The highest amount of particles was found in the liver, followed by the lungs and spleen (data shown in Supplementary Fig. S5).

In contrast to the biodistribution, the transfection capacity clearly differed between lipoplexes carrying respectively unmodified and nucleoside-modified mRNA. Whereas rather low mRNA expression was detected in the lungs for unmodified mRNA, nucleoside-modified mRNA resulted in much higher fLuc expression in the lungs, spleen and at lower (but detectable) level in the liver and at the injection site. Moreover, we were also able to detect mRNA expression in the inguinal lymph nodes indicating that mRNA expression also occurs in organs where T cell activation takes place. As said, fLuc activity in the liver was low, showing that a high lipoplex accumulation (as seen in the liver; see Supplementary Fig. S5) does not result in a high transfection.

When we compared fLuc expression levels in the isolated organs (Fig. 5A–B) we observed that mRNA expression was significantly

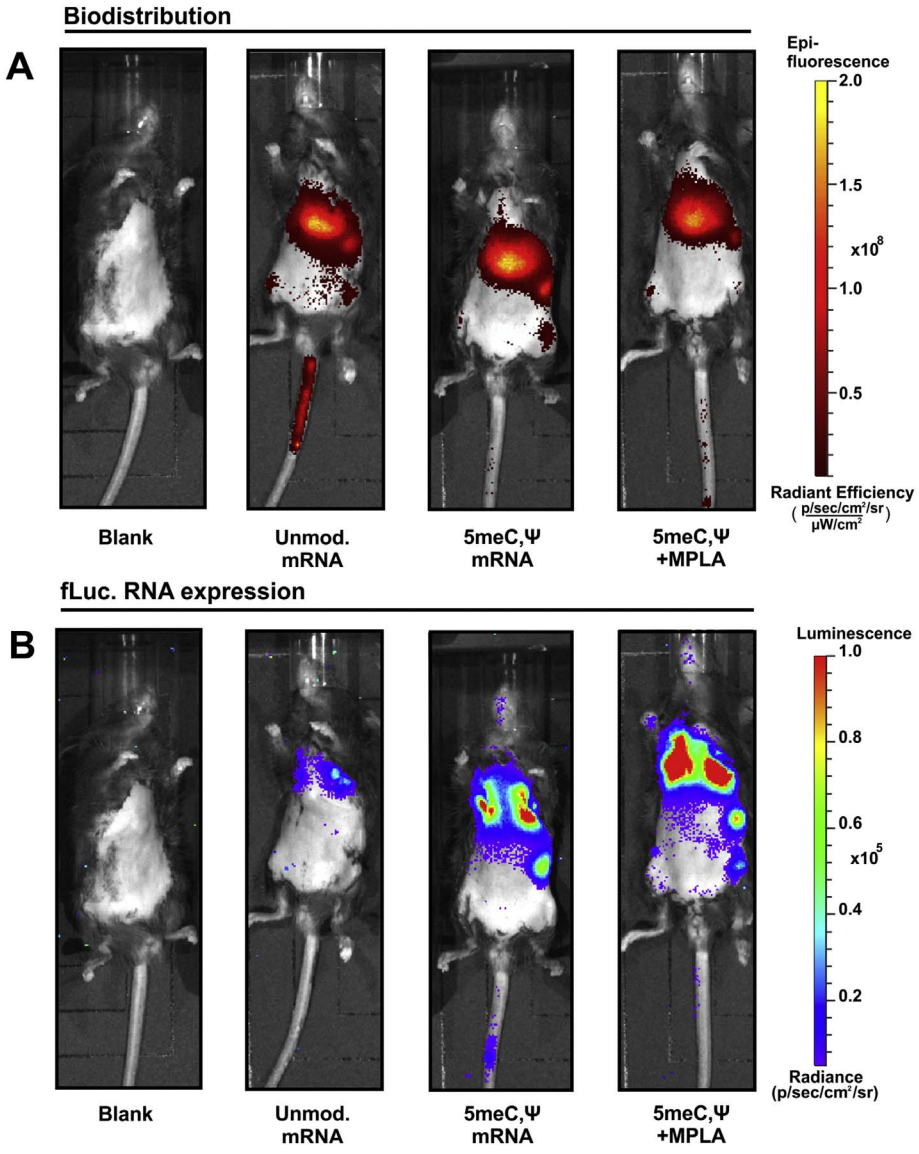

Fig. 4. Biodistribution and *in vivo* transfection after systemic delivery of mRNA lipoplexes. Representative whole body images of C57BL/6 mice demonstrating (A) the biodistribution (DiR fluorescence) of the different mRNA lipoplexes and (B) mRNA expression (fLuc) 5–6 h after injection of DiR labelled fLuc mRNA lipoplexes (n = 9–12). Fluorescence and bioluminescence imaging were performed on the same mice.

increased when using nucleoside-modified mRNA: up to 40 times in the lungs and up to 20 times in the spleen. In agreement with our *in vitro* data (Fig. 3), we also noticed higher transfection efficiency when mRNA lipoplexes carrying both nucleoside-modified mRNA and MPLA were used. This indicates that our *in vitro* BM-DC model is a valuable tool to screen the transfection capacity of nanoparticle formulations before performing more extensive *in vivo* studies.

2.3.2. Cellular uptake of mRNA lipoplexes by APCs in situ

For mRNA lipoplexes to be of value for vaccination purposes, it is important that they are taken up by APCs (like DCs and macrophages) after systemic administration. Therefore, we investigated the mRNA lipoplex uptake in $CD11c^+$ (DCs) and $F4/80^+$ (macrophages) cells within the different organs (lungs, spleen and liver), 12 h after i.v. injection of lipoplexes carrying nucleoside-modified mRNA (Fig. 6). Similar to the biodistribution data (Fig. 4A), no differences were observed between the mRNA lipoplexes (Supplementary Fig. S6). About one-third of the $CD11c^+$ cells (35.5%) and about half of the population of $F4/80^+$ cells (51.0%) became loaded with the DiR labelled mRNA lipoplexes in the lungs. Only a small proportion of lung epithelial ($CD326^+$, 8.8%) and endothelial cells ($CD146^+$, 12.7%) were particle-loaded (Supplementary Fig. S7). Also in the spleen and the liver, $CD11c^+$ (32.8% in spleen and 61.8% in liver) and $F4/80^+$ cells (56% in spleen and 75.5% in liver) took up the mRNA lipoplexes. This illustrates that the mRNA lipoplexes are mainly cleared by DCs and macrophages and are as such expected to favor T cell priming.

2.4. Safety evaluation of systemically delivered mRNA lipoplexes

While the purpose of the mRNA lipoplexes is to induce an adequate immune activation, it remains critical to avoid major organ inflammation and toxicity. Therefore, the safety of the different mRNA lipoplexes was evaluated by means of a histopathological analysis of the lipoplex-targeted organs (*i.e.* lungs, liver and spleen). Fig. 7 shows organ sections of the differently treated animals 24 h post-injection, which were stained with hematoxylin and eosin, and examined for tissue inflammatory reactions by a pathologist in a blinded manner. Importantly, no significant pathological changes were identified in any of the groups. All organs showed normal tissue morphologies, without any signs of necrosis or apoptosis. Furthermore, no abnormalities were detected on external examination, and examination of the organs *in situ*.

2.5. Immune activation by systemically delivered mRNA lipoplexes

To address the stimulatory capacity of the different mRNA lipoplex formulations *in vivo*, we performed a flow cytometric analysis of the

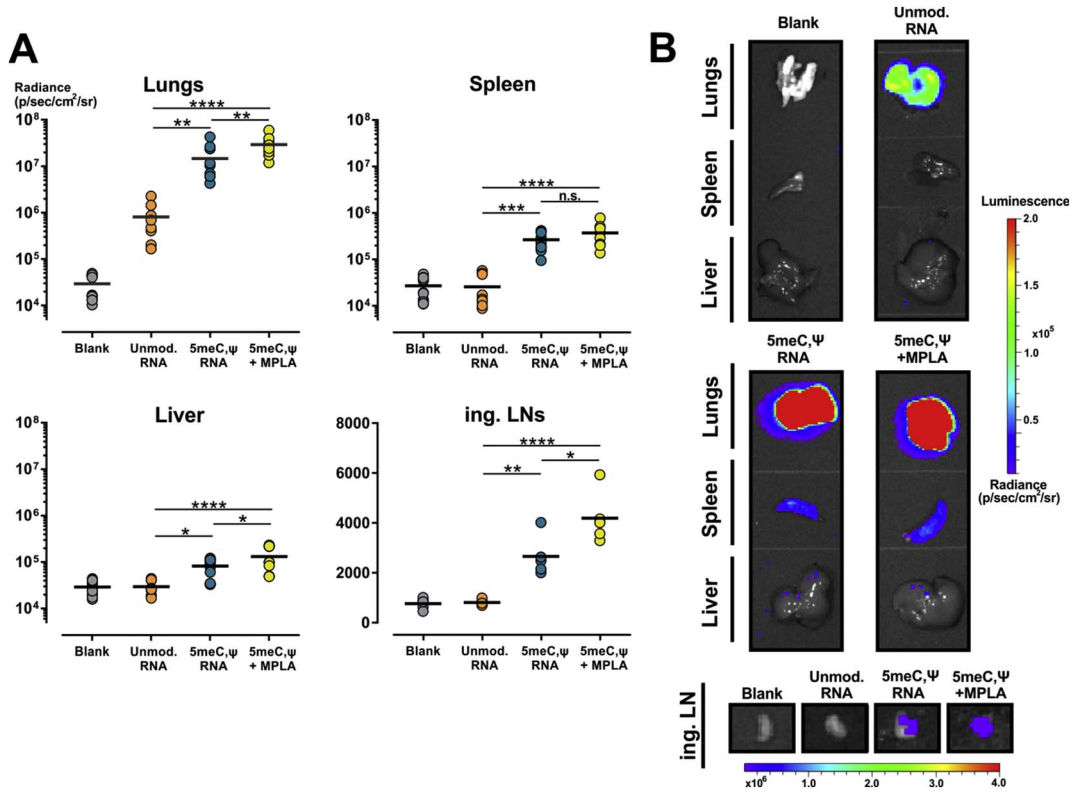

Fig. 5. mRNA expression levels in isolated organs after systemic delivery of mRNA lipoplexes. Bioluminescence imaging of isolated organs (*i.e.* lungs, spleen, liver and inguinal lymph nodes) 5–6 h after injection of mRNA lipoplexes (A) Graphs summarize the bioluminescence measurements obtained in 4 independent experiments (n = 9–12). fLuc expression results in the inguinal lymph nodes are a summary of 2 independent experiments (n = 5). (B) Representative bioluminescence images of isolated organs.

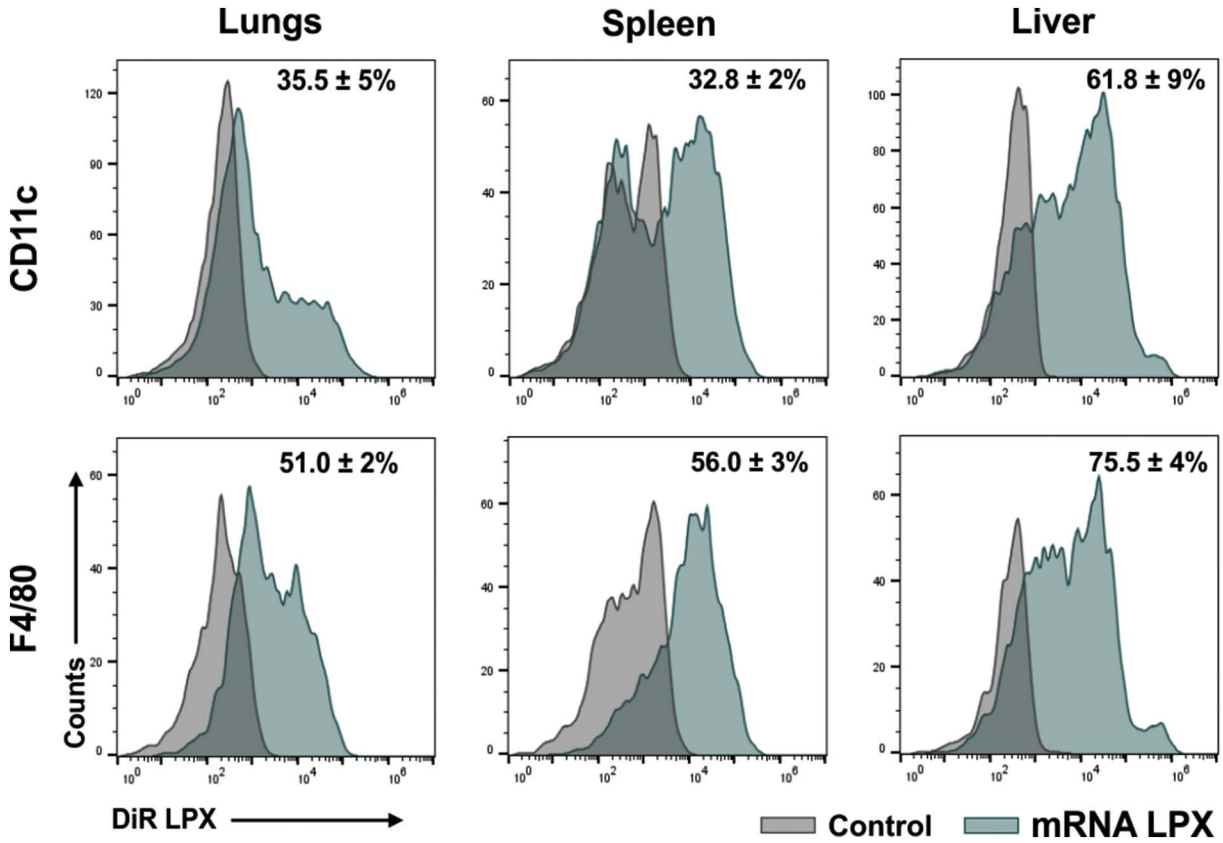

Fig. 6. Uptake of mRNA lipoplexes by APCs. In the isolated organs (lungs, spleen and liver), a major fraction of the CD11c$^+$ cells (DCs) and F4/80$^+$ cells (macrophages) took up lipoplexes carrying nucleoside-modified mRNA. Untreated mice served as controls. Images show representative histograms of the mRNA lipoplex uptake (DiR) in the CD11c$^+$ (DCs) and F4/80$^+$ (macrophages) cell populations. The mean percentage of lipoplex-containing APCs is given in the right top corner of each histogram (n = 3).

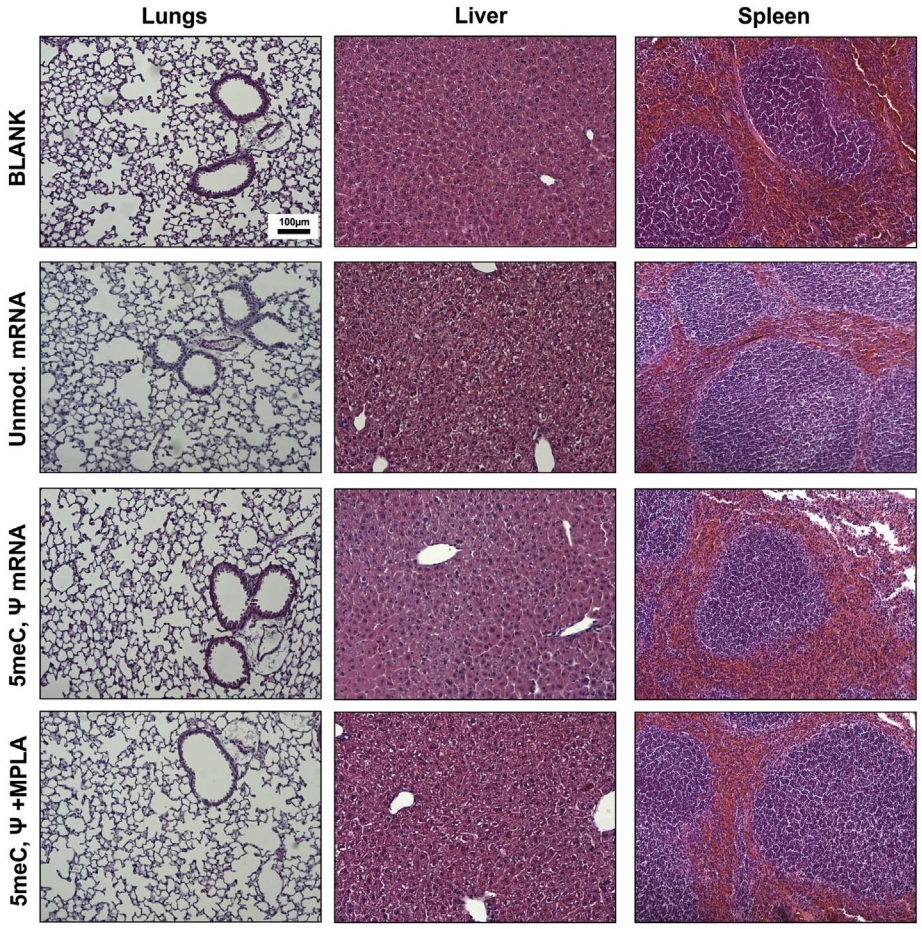

Fig. 7. Histopathological analysis of lungs, liver and spleen after systemic delivery of mRNA lipoplexes. Representative images are shown of organ sections stained with hematoxylin and eosin 24 h post-injection of the different mRNA lipoplexes.

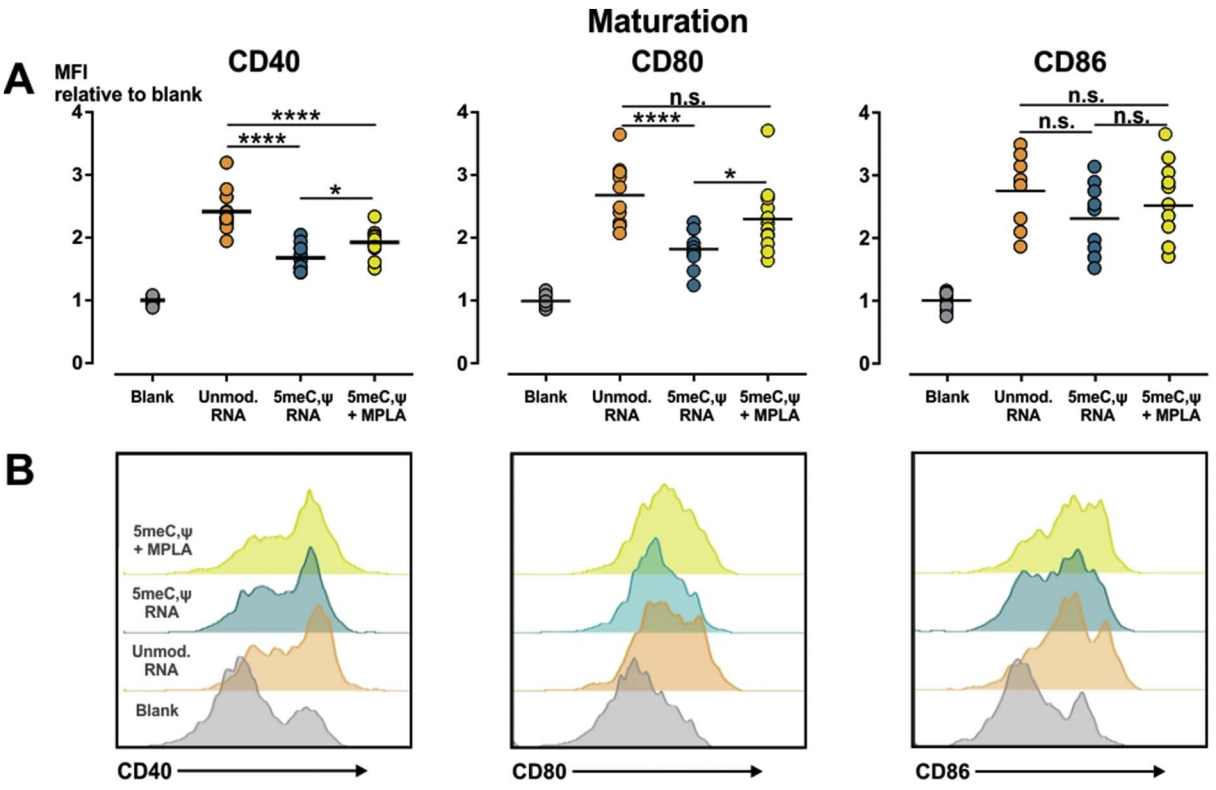

Fig. 8. DC activation capacity of mRNA lipoplexes after systemic delivery in mice. Graphs summarize 4 independent experiments, measuring the upregulation (fold change in MFI) of activation markers in $CD11c^+$ splenocytes (relative to untreated mice) 24 h post-injection (n = 12). Representative histograms of CD40, CD80 and CD86 expression in $CD11c^+$ splenocytes.

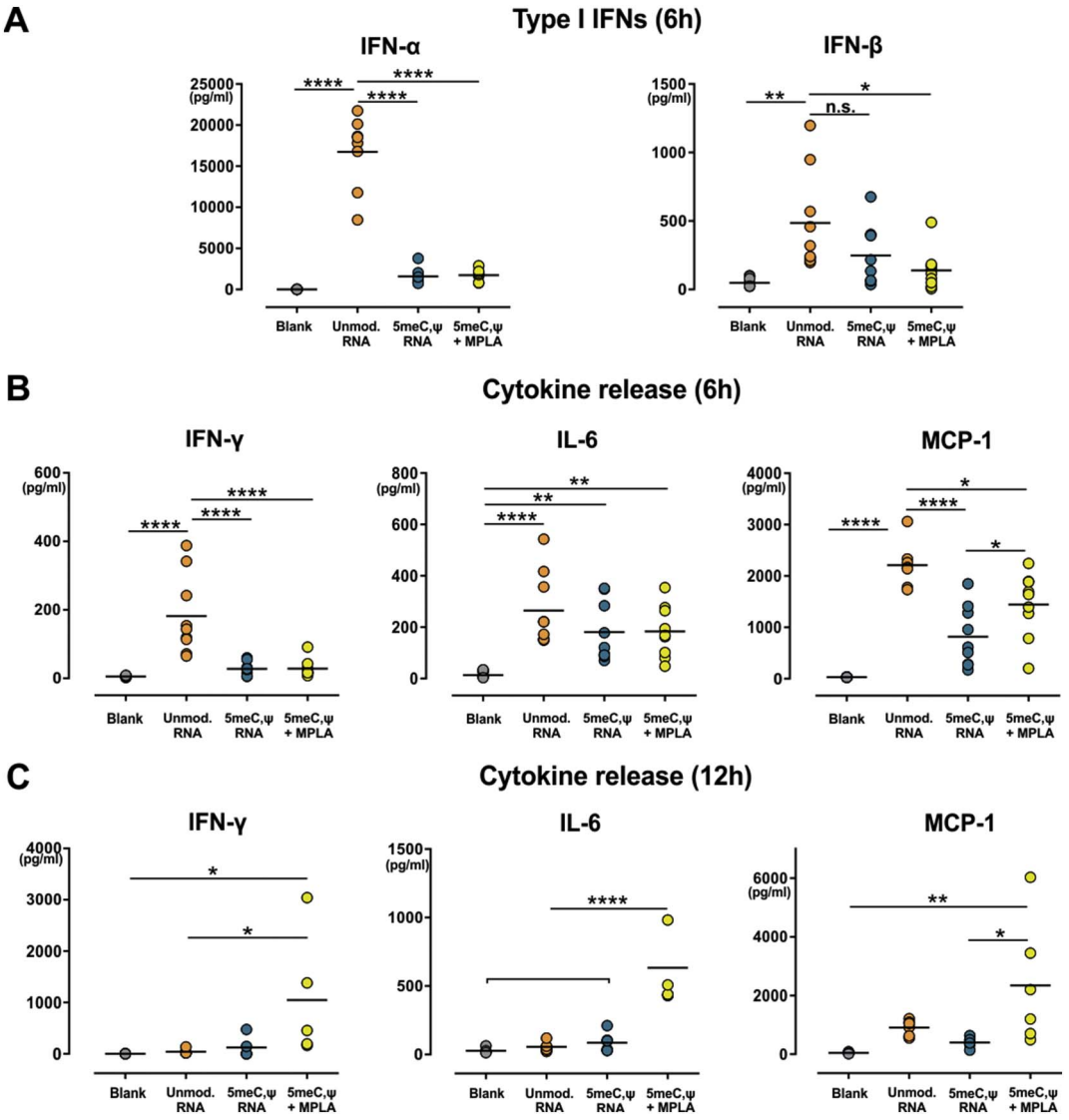

Fig. 9. Cytokine production after systemic delivery of the mRNA lipoplexes. Serum samples were collected from mice sacrificed at different time points (6 h and 12 h post-injection of mRNA lipoplexes) and screened for the release of inflammatory cytokines. In panel (A), graphs summarize the release of the type I IFNs (IFN-α and IFN-β) at 6 h post-injection of three independent experiments (n = 9). The levels of the cytokines IFN-γ and IL-6 and the chemoattractant MCP-1, are shown in panel (B) and (C) for respectively 6 h and 12 h post-injection. In panel (B), the graphs combined the results of three independent experiments (n = 9). In panel C, the graphs are the result of 2 independent experiments (n = 6). No significant differences were detected for the other screened cytokines.

activation status of $CD11c^+$ cells in the spleen (Fig. 8), and quantified the release of type I IFNs and other inflammatory cytokines in blood collected at different time points (Fig. 9).

24 h post-injection, unmodified mRNA lipoplexes induced the highest up-regulation (respectively 2.4, 2.7 and 2.7-fold) of the activation markers CD40, CD80 and CD86 relative to the control mice. A lower but still significant up-regulation of the activation markers (1.7, 1.8 and 2.3-fold) was found in mice treated with modified mRNA. Interestingly, by co-encapsulation of MPLA the lower activation capacity of nucleoside-modified mRNA could, in part, be compensated (1.9, 2.3 and 2.5-fold up-regulation of CD40, CD80 and CD86).

In blood samples collected 6 h post-injection, we measured the production of the type I IFNs; IFN-α and IFN-β. This time-point was chosen based on previous reports showing peak levels of IFN-α 6 h after the i.v. administration of mRNA lipoplexes [19,24]. Lipoplexes with unmodified mRNA induced a very high release of IFN-α with concentrations up to 20 ng ml^{-1} in serum, whereas markedly lower levels (1.5 ng ml^{-1}) were detected when nucleoside-modified mRNA was used (Fig. 9A). Similar trends can be observed in the release of IFN-β. These data confirm that the incorporation of pseudouridine and 5-methylcytidine in the mRNA construct can strongly reduce the induction of type I IFNs *in vivo*.

Additionally, we measured a panel of 13 inflammatory cytokines and chemokines (IL-1α, IL-1β, IL-6, IL-10, IL-12p70, IL-17A, IL-23, IL-27, MCP-1, IFN-β, IFN-γ, TNF-α, and GM-CSF) in serum. Fig. 8B and C summarize the data for the cytokines which were clearly elevated compared to the cytokine levels in control mice 6 h or 12 h after injection of the mRNA lipoplexes. After 6 h, a significant release of IFN-γ, IL-6 and MCP-1 (CCL2), a chemo-attractant which mediates the recruitment and infiltration of monocytes and lymphocytes, was detected in mice treated with mRNA lipoplexes. The production of these mediators was higher at 6 h after i.v. injection when using unmodified mRNA. In contrast, we found the highest release of IFN-γ, IL-6 and MCP-1 in the mice treated with the combination of modified mRNA and MPLA at 12 h after injection. Interestingly, these data show that by including MPLA into the formulation, a similar immune activation and inflammatory cytokine response could be obtained as when using unmodified mRNA, but with a different timing of adjuvant activity and without the strong induction of IFN-α. Other than for IFN-γ, IL-6 and MCP-1, no statistically significant differences were observed for the

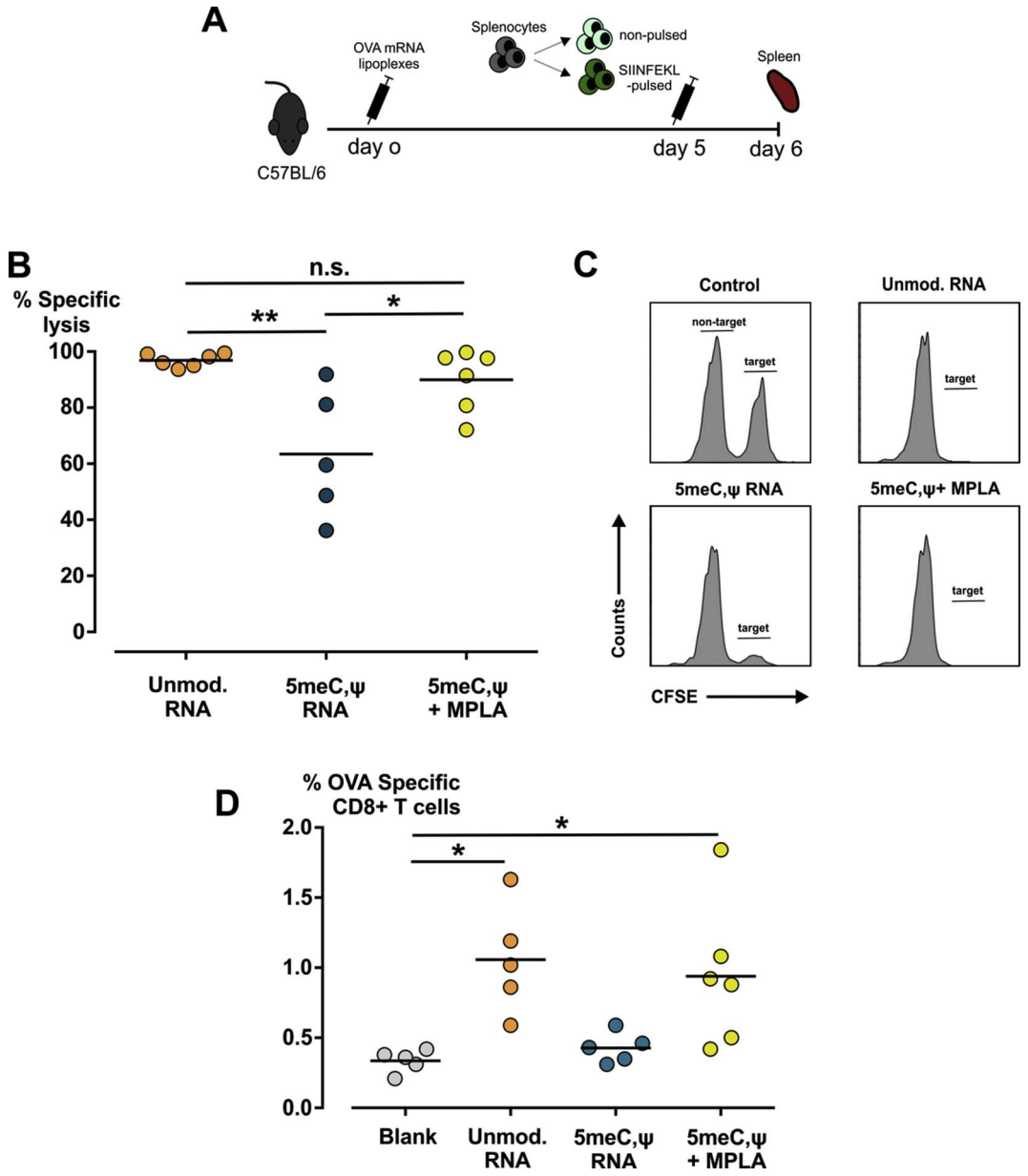

Fig. 10. Capacity of the mRNA lipoplexes to induce cytotoxic T cell responses *in vivo*. (A) Mice were immunized with OVA-encoding mRNA lipoplexes. 5 days later, an *in vivo* CTL assay was performed and OVA-specific CD8 + T cells were measured using a tetramer staining. (B) The graph depicts the antigen-specific lysis of target cells compared to non-target cells, summarizing two independent experiments (n = 5–6). Representative histograms showing the relative distribution of target to non-target cells are provided in panel (C). (D) Graph summarizes the percentages of OVA SIINFEKL specific $CD8^+$ T cells (spleen) of two independent experiments.

other investigated cytokines and chemokines. The cytometric bead array was also performed on blood samples collected 24 h after injection, but at this time point, all of the cytokine levels had returned to baseline (except for MCP-1, Supplementary Fig. S8).

2.6. Induction of antigen-specific T cell immunity

Finally, we performed an *in vivo* cytotoxicity assay to score the capacity of the mRNA lipoplex formulations to prime functional antigen-specific cytotoxic T cells. For this, mice were immunized with lipoplexes loaded with mRNA encoding chicken ovalbumin (OVA) as a model antigen. Five days after immunization, the mice were challenged with syngeneic splenocytes that were either untreated (non-target cells) or pulsed with the OVA-derived peptide SIINFEKL (target cells). The next day, the antigen-specific lysis of the target cells was measured. Mice vaccinated with unmodified mRNA showed complete lysis (97 ± 2%) of the target population (Fig. 10). Reduced antigen-specific lysis (63 ± 23%) was found in mice immunized with nucleoside-modified mRNA, indicating that the loss in DC activation (as mentioned in Section 2.5) influences the vaccine efficacy. Most importantly, combining nucleoside-modified mRNA with MPLA induced strong OVA specific T cell responses also resulting in almost complete lysis (90 ± 11%) of the target cells. This trend is also observed in the numbers of antigen-specific cytotoxic T cells; the expansion of OVA SIINFEKL $CD8^+$ T cells observed in mice vaccinated with lipoplexes containing nucleoside-modified mRNA and MPLA was similar as when using unmodified mRNA, whereas without MPLA no significant levels were measured. With these data, we provide proof that we can restore the capacity of nucleoside-modified mRNA lipoplexes to prime functional antigen-specificic cytotoxic T cells by combining this with an immune adjuvant such as MPLA without provoking a type I IFN response.

3. Discussion

In this study we report on DOTAP-cholesterol mRNA lipoplexes for the purpose of therapeutic cancer vaccination. For the first time we investigated whether the combined use of nucleoside-modified mRNA and TLR agonists could be a promising strategy for mRNA vaccination purposes.

In an BM-DC *in vitro* model [42], we first screened lipoplex formulations for the intracellular delivery of mRNA by varying the lipid composition, lipid-to-mRNA ratio, and mRNA construct. As these particles are aimed for intravenous administration, it is of the utmost importance that they retain their properties in serum-containing media. Indeed, upon systemic administration mRNA lipoplexes encounter a variety of biomolecules in the bloodstream, which can induce structural lipid rearrangements and dynamic changes in composition of the lipoplex surface, potentially affecting the mRNA delivery [43–46]. By using cholesterol instead of DOPE, we obtained mRNA lipoplexes that remained stable and preserved their transfection efficiency in serum. This corresponds to earlier studies in which the same "helper" lipids, DOPE *versus* cholesterol, were investigated for pDNA delivery [45,47,48]. Furthermore, we did not include a PEGylated lipid in our formulation. Nanoparticles are often PEGylated to reduce opsonisation and as such avoid unspecific uptake by the mononuclear phagocyte system. One could assume that PEGylation could potentially affect the uptake of mRNA lipoplexes by APCs [49,50]. Our data showed that the incorporation of PEGylated lipids seems redundant as the mRNA lipoplexes remain stable in serum: they protect the mRNA from degradation, pre-mature release of the mRNA is not observed while the lipoplexes do not aggregate. As expected, we observed that the mRNA lipoplexes were rapidly cleared from the blood by phagocytic cells and accumulated in the lungs, spleen, liver and bone marrow.

A most prominent effect with respect to both transfection efficiency and localization of mRNA expression was observed when mRNA constructs, respectively unmodified- and nucleoside-modified mRNA, were compared side-by-side. The nucleoside-modified mRNA incorporates 5′-„methylcytidine and pseudouridine in the transcript, which improves the mRNA stability and increases the translation capacity [34]. Without these modifications, mRNA binds to several endosomal and cytoplasmic pattern recognition receptors initiating distinct antiviral pathways regulated by type I IFN and programmed to degrade the mRNA and inhibit its translation [32,35,51]. Several studies using transgenic type I IFN reporter mice identified macrophages, conventional DCs and especially plasmacytoid DCs as the major producers of type I IFNs. Both the cell types involved and the strength and kinetics of the IFN-α/β action seem to differ for lungs, spleen and liver [52–54]. This probably explains why we could not only observe a more pronounced expression in the lungs, but also detected expression levels in the spleen, liver and lymph nodes when nucleoside-modified mRNA was used. According to these findings, we conclude that type I IFNs might not only influence the total mRNA expression efficiency of the mRNA lipoplexes, but also affect the organ and the specific cells that will finally express the mRNA. Alternatively, Kranz and colleagues described that the systemic administration of negatively-charged mRNA lipoplexes at a low lipids-to-mRNA ratio, where not all the mRNA was encapsulated, resulted in the specific transfection of APCs in the spleen [24]. Similar to our study, at higher lipid-to-mRNA ratio's resulting in complete mRNA packaging, a seemingly less favorable distribution with a relatively high lung expression was observed. The question remains which intermediate effects are responsible for this shift in mRNA expression when adjusting the lipid-to-mRNA ratio: the particle's surface charge, particle size, differences in structural organization of mRNA-lipid complexes, total lipid-mRNA dose, *etc*. Note that the high expression levels in lung APCs could become a favorable strategy to treat lung cancer [55–58].

Nucleoside-modified mRNA is becoming a golden standard when the aim is to produce high levels of a therapeutic protein [59–61]. However, when it comes to cancer immunotherapy, it is of crucial importance to provoke an adequate immune activation. Indeed, recent studies have identified the mRNA's "self-adjuvant" effect, mediated by the type I IFN response, as the main driver for effective T cell activation and anticancer immunity [19,24,25]. Diminishing the type I IFN signaling in these studies negatively impacted the capacity to activate DCs and induce adaptive immunity. In sharp contrast, De Beuckelaer et al. rather demonstrated that type I IFNs severely hamper the vaccine efficacy of DOTAP-DOPE mRNA lipoplexes upon subcutaneous, intradermal and intranodal administration [27]. In a recent review they postulated that type I IFNs, depending on the timing between type I IFN signaling and T cell priming, can induce an opposing role on T cell modulation [26]. Likewise, Pepini and colleagues stated that the early type I IFN response should be minimized to increase the primary expression of self-amplifying mRNA vaccines [29]. These contradictory findings once again underline the importance to optimally balance the dynamics and kinetics of mRNA expression and DC activation to achieve a successful vaccine efficacy, which was also highlighted in a recent review by Iavarone et al. [28]. Strikingly, in the *in vitro* BM-DC model the mRNA lipoplexes failed to induce DC maturation and no release of type I IFNs or other inflammatory cytokines was detected. To explain this, it is important to consider that BM-DCs are artificially generated DCs that do not fully correspond to their most abundant *in vivo* counterparts. As such, Dearman et al. showed that BM-DCs lack responsiveness to polyuridylic acid (poly-U, TLR7 ligand) and polyinosinic-polycytidylic acid (poly-(I:C), TLR3 ligand), which suggests that BM-DCs might not express the most important TLRs involved in the recognition of mRNA [62]. Indeed, whereas no type I IFN response was detected *in vitro*, the intravenous delivery of unmodified mRNA was marked by the rapid induction of type I IFNs mediating an adequate DC activation, which nicely corresponds to the results described by Kranz et al. and Broos et al. By delivering nucleoside-modified mRNA *in vivo*, we could observe a strong reduction (but not a complete disappearance) in the production of type I IFNs. Nonetheless, this merely provoked a low activation of the targeted APCs, which ultimately affected the capacity of the mRNA lipoplexes to induce functional T cell responses.

To compensate for the loss in immunogenicity, we investigated whether nucleoside-modified mRNA could be co-delivered with the TLR4 agonist MPLA. While the adjuvant effect of TLR agonists for peptide and protein vaccines has been well studied, only a few studies have evaluated the combination of unmodified mRNA with TLR agonists (lipopolysaccharide, poly-(I:C) MPLA) [25,41,63]. Initial mRNA vaccine studies have focused on the direct administration of naked antigen-encoding mRNA. Back then it was shown that the co-delivery of mRNA with TLR agonists completely abrogated the uptake of the naked mRNA by local DCs *via* macropinocytosis, resulting in a complete loss of transfection efficiency [41,63]. For the first time we show that co-delivering a TLR agonist (MPLA) with nucleoside-modified mRNA lipoplexes is feasible and can be used to promote innate immune activation, and this without compromising the transfection efficiency. We demonstrate that this a safe approach to induce effective T cell immunity, which can compete with mRNA lipoplexes using unmodified mRNA.

In summary, we have shown clear evidence that a thorough *in vitro* characterization of the particle properties with respect to cargo protection and stability in biologically relevant media, is of great relevance to optimize mRNA lipoplexes for *in vivo* use. Subsequently, we showed that, despite a successful transfection of APCs by DOTAP-cholesterol mRNA lipoplexes, upon cellular entry type I IFNs induced by unmodified mRNA restricted the mRNA expression. Using nucleoside-modified mRNA reduces the intracellular immune recognition, and as such avoids the strong release of type I IFNs. We showed that this clearly improved the translational potential of the mRNA lipoplexes, and provided a more widespread APC contribution. Finally, we provided the proof of concept that the "diminished self-adjuvant" effect of nucleoside-modified mRNA can be compensated by co-delivery of MPLA. We hope that the approach of combining nucleoside-modified

mRNA with well-known adjuvants will catalyze further improvements in the efficiency and safety of mRNA vaccines.

4. Materials and methods

4.1. Cell culture and mice

Female C57BL/6 mice were purchased from Envigo (Gannat, France) and housed in an SPF facility. All animal experiments were conducted according to the regulations of the Belgian law and approved by the local Ethical Committee. To generate primary murine bone marrow-derived DC (BM-DC) cultures, 7 weeks old mice were sacrificed and bone marrow was flushed from the femur and tibia. The collected bone marrow was cryopreserved in FetalClone™ I serum (FCI, Batch n°AXD36551, HyClone™, Pierce, Rockford, IL, USA) with 2% glucose (Sigma-Aldrich, Bornem, Belgium) and 10% DMSO (Sigma-Aldrich). To start a culture of BM-DCs, bone marrow of one hind leg was thawed and the cells were seeded in a 100 mm Not TC-Treated polystyrene Culture Dish (Corning®, Amsterdam, The Netherlands). Cells were cultured in RPMI 1640 medium (Gibco-Invitrogen, Merelbeke, Belgium) supplemented with penicillin/streptomycin/L-glutamine (1%, Gibco-Invitrogen), β-mercaptoethanol (50 μM, Gibco-Invitrogen) and 5% FCI serum. GM-CSF (20 ng ml^{-1}, Peprotech, Rock Hill, NJ) was used to promote differentiation of the monocytes into BM-DCs. On day 3 of the culture, an additional 15 ml culture medium containing GM-CSF (40 ng ml^{-1}) was added. After two more days, cells were collected by centrifugation (5 min at 300*g*), resuspended in GM-CSF supplemented culture medium at 10^6 cells ml^{-1} and seeded in 24 well plates for experiments (5×10^5 cells per well). For the *in vivo* experiments, 7 weeks old C57BL/6 mice were used.

4.2. mRNA constructs

Unmodified and nucleoside-modified (5meC, Ψ) mRNA encoding firefly luciferase (fLuc), and the Cy5 labelled mRNA construct (5meC, Ψ) encoding for eGFP were purchased from TriLink (San Diego, CA). For the immunization studies, a truncated form of ovalbumin (tOVA) fused to the first 80 amino acids of the invariant chain (Ii80) was produced by *in vitro* mRNA transcription from pGEM-Ii80tOVA plasmids [64]. The plasmids were purified using a QIAquick PCR purification kit (Qiagen, Venlo, The Netherlands) and linearized using the *Spe* I restriction enzyme (Promega, Leiden, The Netherlands). Linearized plasmids were used as templates for the *in vitro* transcription reaction using the T7 MegaScript kit, including an Anti-Reverse Cap Analog (ARCA) and Poly (A) tailing reagents (Ambion, Life Technologies, Ghent, Belgium). For the transcription of modified mRNA, cytidine and uridine nucleotides were 100% replaced by 5-methylcytidine and pseudouridine (TriLink). The resulting mRNAs were purified by DNase I digestion, precipitated with LiCl and washed with 70% ethanol. The mRNA concentration was determined by measuring the absorbance at 260 nm. mRNAs were stored in small aliquots at − 80 °C at a concentration of 1 μg $μl^{-1}$.

4.3. mRNA lipoplex preparation

The lipids DOTAP (1,2-dioleoyl-3-trimethylammonium-propane), cholesterol and DOPE (1,2-dioleoyl-sn-glycero-3-phosphoethanolamine) were purchased from Avanti Polar Lipids (Alabaster, USA). Cationic liposomes of DOTAP-DOPE (1:1 M ratio) and DOTAP-cholesterol (2:3 M ratio) were prepared by transferring the appropriate amounts of lipids, dissolved in chloroform into a round-bottom flask. The chloroform was evaporated under nitrogen, after which the lipid film was rehydrated in HEPES buffer (20 mM, pH 7.4, Sigma-Aldrich) to obtain a final lipid concentration of 12.5 μmol ml^{-1}. The resulting cationic liposomes were sonicated until the dispersion became clear in a bath sonicator (Branson Ultrasonics, Dansbury, USA). Then, they were mixed with mRNA to obtain mRNA lipoplexes at different cationic lipid-to-mRNA charge ratios. Full mRNA complexation was seen at a (nitrogen/phosphate; N/P) ratio of 2.5, and hence used for further experiments. The obtained mRNA lipoplexes were incubated for 15 min at room temperature before use. For the co-encapsulation of MPLA in the mRNA lipoplexes, 0.5 mol% of the total lipid amount was replaced by MPLA (TLR4 agonist, Sigma-Aldrich). For the biodistribution studies, 1 mol% of the total lipid amount was replaced by the lipophilic DiR fluorescent dye (Thermo Scientific), respectively. The incorporation of MPLA or DiR did not influence the physicochemical properties of the mRNA lipoplexes. mRNA lipoplexes for *in vivo* use were prepared in an isotonic HEPES buffer containing 5% glucose.

4.4. Physicochemical characterization of the mRNA lipoplexes

mRNA lipoplexes prepared at different N/P ratios in HEPES buffer were subjected to a size and zeta potential quality control using a Malvern Zetasizer nano-ZS (Malvern Instruments Ltd., Worcestershire, UK). To examine the complexation of mRNA to the liposomes and the stability of this interaction in serum-containing medium, mRNA lipoplexes were diluted and incubated in 50% FCI serum or 50% human serum. After 2 h incubation at 37 °C, Ambion loading buffer (Ambion) was added and mixtures were loaded into a 1% agarose gel in TBE buffer, to which GelRed (Biotium, Hayward, CA) was added for visualization of the mRNA. The gel was run for 30 min at 100 V and imaged under UV light. Samples containing only (unpackaged, *i.e.* so named 'naked') mRNA, only serum or serum together with naked mRNA, were run as controls. A molecular weight marker with bands at a range of 0.25 to 10 kb was included to provide size determination of the RNA (Promega, Leiden, The Netherlands).

To predict the colloidal stability of mRNA lipoplexes in serum, lipoplexes containing Cy5 labelled mRNA were incubated up to 24°h in 90% human serum at 37 °C. Subsequently their size distribution was evaluated by fluorescence single particle tracking (fSPT) microscopy. fSPT allows to monitor the diffusion of fluorescently labelled nanoparticles in biological fluids [65]. By recording high-speed confocal movies of individually moving particles, motion trajectories of single particles can be visualized and their size distribution can be calculated. fSPT measurements on mRNA lipoplexes were performed as follows; first, 20 μl of Cy5-labelled mRNA lipoplexes was diluted in human serum (1:25) and incubated for 2 h, 6 h or 24 h at 37 °C, after which 5 μl was added to 45 μl of human serum. The samples were then transferred to a black coated 96 well plate and placed on a swept-field confocal microscope (LiveScan Swept Field Confocal Microscope System; Nikon, Brussels, Belgium) equipped with a Plan Apo 60 × 1.0 NA oil immersion objective lens (Nikon) and a fast and sensitive EMCCD camera (Ixon Ultra 897; Andor Technology, CT, USA). The microscope was focused 20 μm above the bottom of the well plate and the Cy5-labelled mRNA lipoplexes were excited with a solid-state 125 mW 640 nm (Agilent Technologies, CA, USA) laser. For each sample, 20 movies of about 100 frames each were recorded at different random locations within the sample.

4.5. In vitro evaluation of mRNA lipoplexes

The *in vitro* experiments were performed on BM-DCs at day 6 of cell culture. The day before transfection, cells were seeded in 24 well plates at 5×10^5 cells per well, and grown in the cell culture medium with 5% FCI serum. mRNA lipoplexes (1 μg mRNA per 5×10^5 cells) were added directly to the cells in the complete cell culture medium. For the fLuc activity, cells were transfected with mRNA lipoplexes carrying nucleoside modified mRNA (5meC, Ψ) or unmodified fLuc mRNA (TriLink). After 5–6 h, all cells were collected from the wells and washed in PBS (Gibco-Invitrogen). Subsequently, cells were lysed with Cell Culture Lysis Reagent (Promega) and analyzed for fLuc expression using the Luciferase Assay Kit (Promega) according to the manufacturer's instructions. The bioluminescence (relative light units, RLU) was

measured using a GloMax luminometer (Promega). The protein content of each sample was determined using the Micro BCA protein assay kit (Thermo Scientific, Cramlington, UK). The results are expressed as RLU per milligram of protein. The potency of the mRNA lipoplexes in triggering the activation of BM-DCs was analyzed by measuring the up-regulation of the maturation surface markers CD40, CD80 and CD86. Respectively untreated cells and cells stimulated with *E. coli*-derived lipopolysaccharide (0.2 μg ml^{-1} LPS, Sigma-Aldrich) were used as negative and positive controls. 24 h after the addition of mRNA lipoplexes (fLuc mRNA), the cells were collected and washed with PBS. Subsequently, cells were stained with a fixable viability dye eFluor® 450 (eBioscience) according to the manufacturer's instructions, incubated with Fc receptor block (anti-CD16/32) to block non-specific FcR binding (BD Biosciences, Erembodegem, Belgium), and surface stained for CD11c-APC (clone N418) and, CD40-FITC (Clone HM40-3), CD86-FITC (clone CL1) or CD80-PE/Cy7 (clone 16-10A1, all eBiosciences) for 30 min at 4 °C. After additional washing steps, the cells were analyzed by flow cytometry using a CytoFLEX (Beckman Coulter, Krefeld, Germany) and analysis was performed using FlowJo software (FlowJo, OR, USA). For the transfection with Cy5-labelled nucleoside modified mRNA (5-methylcytidine, pseudouridine, TriLink), cells were seeded in 35 mm MatTek glass bottom culture dishes (MatTek Corporation, MA, USA) on day 5 of the culture, and transfected and imaged on day 6. Confocal microscopy images of the cells were recorded using a Nikon C1si confocal laser scanning module attached to a motorized Nikon TE2000-E inverted microscope (Nikon Benelux, Brussels, Belgium), equipped with a Plan Apo 60 × 1.0 NA oil immersion objective lens (Nikon).

4.6. Intravenous administration of mRNA lipoplexes

Mice were anesthetized in a ventilated anesthesia chamber with 3% isoflurane in oxygen. Prior to injection, a catheter of polyethylene tubing (Intramedic PE10, BD) containing sterile 0.9% NaCl solution was inserted in the tail vein. After correct placement, lipoplexes with the indicated cargo diluted in sterile 5% glucose HEPES buffer were slowly injected (250 μl containing 10 μg mRNA per mouse).

4.7. Bioluminescence- and fluorescence imaging

Lipoplexes containing fLuc mRNA (TriLink) with 1 mol% of the total lipid amount replaced by the lipophilic DiR fluorescent dye were used for these experiments. Five to 6 h after the injection of the mRNA lipoplexes, mice were anesthetized and abdomen and chest were depilated with hair removal cream. Subsequently, VivoGlo™ Luciferin (Promega) was administered intraperitoneally in a volume of 100 μl (33 mg ml^{-1}) per mouse. After 10 min bioluminescence images and fluorescence images (Far-red region) were acquired by the IVIS lumina II system (PerkinElmer, Waltham, MA). The acquisition time was 10 min for bioluminescence and 1 s for fluorescence. Luminescence and fluorescence were quantified using the Living Image software (PerkinElmer).

4.8. In vivo cellular uptake, maturation and cytokine determination

Mice were i.v. injected with DiR labelled- or unlabelled mRNA lipoplexes for the evaluation of the cellular uptake or DC maturation, respectively. After 24 h, mice were sacrificed and spleen, lungs, and liver were harvested and processed into single cell suspensions. Splenocytes were obtained by pressing the spleens through a 40 μm cell strainer (Corning, NY, USA). Liver and lungs were dissociated using a Tissue Dissociation Kit according to the manufacturer's instructions (Miltenyi Biotec, Leiden, The Netherlands). Erythrocytes were removed by addition of a red blood cell lysis buffer (Biolegend, San Diego, CA).

The maturation status of $CD11c^+$ cells in the spleen was analyzed by measuring the up-regulation of the maturation surface markers CD40, CD80 and CD86. The uptake of lipoplexes by specific cell types in the different organs, $F4/80^+$ (macrophage), $CD11c^+$ (DC), $CD146^+$ (endothelial) and $CD326^+$ (epithelial) cells, was measured by analyzing the DiR signal, as a tracer for the mRNA lipoplexes. Single cell suspensions were stained with a fixable viability dye eFluor® 450 (eBioscience) according to the manufacturer's instructions to exclude dead cells from analysis, incubated with Fc receptor block (anti-CD16/32) to block non-specific FcR binding (BD Biosciences, Erembodegem, Belgium), and surface stained with the indicated antibodies during 30 min at 4 °C. Antibodies included CD11c-(APC or FITC), F4/80-FITC (clone BM8), CD146-FITC (clone P1H12), CD326-FITC (clone G8.8), CD40-FITC, CD86-FITC and/or CD80-PE/Cy7 (all eBioscience). After additional washing steps, the cells were analyzed by flow cytometry.

Serum was collected at different time points (6, 12 or 24 h after i.v. injection of the mRNA lipoplexes) and samples were stored at − 20 °C. The production of IFN-α was determined 6 h after injection using the Mouse Platinum IFN alpha ELISA kit (eBioscience). IL-12p70 and IFN-γ release were measured 12 h post-injection, using Ready-SET-Go!® ELISA kits, (eBioscience). A panel of 13 other cytokines, including IL-1α, IL-1β, IL-6, IL-10, IL-12p70, IL-17A, IL-23, IL-27, MCP-1, IFN-β, IFN-γ, TNF-α, and GM-CSF, was quantified using a multiplex assay and performed according to the manufacturer's instructions (LEGENDplex™ Mouse Inflammation Panel, Biolegend).

4.9. Histopathological analysis

The lipoplex-targeted organs, liver, spleen and lungs, were isolated 24 h after injection of mRNA lipoplexes. The organs were fixed immediately in 4% paraformaldehyde in PBS for at least 24 h. The organs were embedded in paraffin, and then sectioned and stained with hematoxylin and eosin (H&E). All slides were examined for tissue inflammatory reactions by a pathologist in a blinded manner.

4.10. In vivo cytotoxic T lymphocyte assay/H-2Kb/SIINFEKL tetramer staining

To investigate the potential of the mRNA lipoplexes with different cargos to induce antigen-specific CTL responses, an *in vivo* CTL assay was performed using ovalbumin (OVA) as a model antigen. For this, mice received i.v. injections with lipoplexes containing tOVA mRNA. 5 days after immunization the animals were challenged i.v. with both target cells and control cells in a 1:1 ratio. The injected cells were splenocytes of untreated C57BL/6 mice that were either labelled with carboxyfluorescein diacetate succinimidyl ester (CFSE) at low intensity ($CFSE^{lo}$ control cells, 5×10^6 cells per injection), or labelled with CFSE at high intensity and additionally pulsed with the peptide SIINFEKL ($CFSE^{hi}$ target cells, 5×10^6 cells per injection). The next day, the mice were sacrificed, spleens were collected, processed into a single-cell suspension, and analyzed for CFSE staining *via* flow cytometry. Untreated mice served as non-immunized controls. The percentage specific lysis of target cells was calculated as $(1 - ((\%CFSE^{hi} / \%CFSE^{lo})_{immunized} / (\%CFSE^{hi} / \%CFSE^{lo})_{non\text{-}immunized}) \times 100\%$.

In addition, a tetramer staining was used for the detection of H-2Kb/SIINFEKL specific T cells. BV450-conjugated H-2Kb/SIINFEKL tetramer (OVA-tetramer) was obtained from the National Institutes of Health (NIH) Tetramer Core Facility. Splenocytes were isolated as described in Section 4.8, incubated with Fc block, and surface stained with CD8a-APC antibody (eBioscience). Dead cells were excluded using a 7-AAD viability stain (eBioscience) and the tetramer staining was performed according to NIH's instructions.

4.11. Statistical analysis

All data are presented as mean ± standard deviation. Presented data are representative for at least 3 independent experiments performed on 3 different days. When data of multiple experiments are

merged into a single graph, this is explicitly mentioned in the figure caption. Statistical analyses were performed using a One-Way ANOVA followed by Tukey's *post hoc* test (GraphPad Prism6, La Jolla, CA, USA). Asterisks indicate statistical significance (*, $p < 0.05$; **, $p < 0.01$; ***, $p < 0.001$).

Acknowledgements

The authors would like to thank George Dakwar, Elisa Zagato, Toon Brans and Karen Peynshaert for their help with the SPT and confocal microscopy experiment. They further wish to thank Dana De Saegher for her help with the experimental work, and Leen Pieters and Heidi Declercq for the sample preparation for the histopathology study. Heleen Dewitte is a postdoctoral fellow of the Research Foundation-Flanders, Belgium (FWO-Vlaanderen). This research is supported by the FWO grants No. G016513N and G0B2814N.

Appendix A. Supplementary data

Supplementary data to this article can be found online at https://doi.org/10.1016/j.jconrel.2017.09.041.

References

[1] N.P. Restifo, M.E. Dudley, S.A. Rosenberg, Adoptive immunotherapy for cancer: harnessing the T cell response, Nat. Rev. Immunol. 12 (2012) 269–281.
[2] P.G. Coulie, B.J. Van den Eynde, P. van der Bruggen, T. Boon, Tumour antigens recognized by T lymphocytes: at the core of cancer immunotherapy, Nat. Rev. Cancer 14 (2014) 135–146.
[3] G.P. Dunn, A.T. Bruce, H. Ikeda, L.J. Old, R.D. Schreiber, Cancer immunoediting: from immunosurveillance to tumor escape, Nat. Immunol. 3 (2002) 991–998.
[4] A. Corthay, Does the immune system naturally protect against cancer? Front. Immunol. 5 (2014) 197.
[5] S. Kreiter, M. Vormehr, N. van de Roemer, M. Diken, M. Lower, J. Diekmann, S. Boegel, B. Schrors, F. Vascotto, J.C. Castle, A.D. Tadmor, S.P. Schoenberger, C. Huber, O. Tureci, U. Sahin, Mutant MHC class II epitopes drive therapeutic immune responses to cancer, Nature 520 (2015) 692–696.
[6] D. Benteyn, C. Heirman, A. Bonehill, K. Thielemans, K. Breckpot, mRNA-based dendritic cell vaccines, Expert Rev. Vaccines 14 (2015) 161–176.
[7] S. Anguille, E.L. Smits, E. Lion, V.F. van Tendeloo, Z.N. Berneman, Clinical use of dendritic cells for cancer therapy, Lancet Oncol. 15 (2014) e257–267.
[8] S. Van Lint, D. Renmans, K. Broos, H. Dewitte, I. Lentacker, C. Heirman, K. Breckpot, K. Thielemans, The ReNAissanCe of mRNA-based cancer therapy, Expert Rev. Vaccines 14 (2015) 235251.
[9] P.J. Tacken, I.J. de Vries, R. Torensma, C.G. Figdor, Dendritic-cell immunotherapy: from ex vivo loading to in vivo targeting, Nat. Rev. Immunol. 7 (2007) 790–802.
[10] C.M. Jewell, S.C.B. Lopez, D.J. Irvine, In situ engineering of the lymph node microenvironment via intranodal injection of adjuvant-releasing polymer particles, Proceedings of the National Academy of Sciences of the United States of America, Vol. 108 2011, pp. 15745–15750.
[11] J.I. Andorko, K.L. Hess, C.M. Jewell, Harnessing biomaterials to engineer the lymph node microenvironment for immunity or tolerance, AAPS J. 17 (2015) 323–338.
[12] H. Dewitte, R. Verbeke, K. Breckpot, S.C. De Smedt, I. Lentacker, Nanoparticle design to induce tumor immunity and challenge the suppressive tumor microenvironment, Nano Today 9 (2014) 743–758.
[13] A. Selmi, F. Vascotto, K. Kautz-Neu, Ö. Türeci, U. Sahin, E. von Stebut, M. Diken, S. Kreiter, Uptake of synthetic naked RNA by skin-resident dendritic cells via macropinocytosis allows antigen expression and induction of T-cell responses in mice, Cancer Immunol. Immunother. 65 (2016) 1075–1083.
[14] J.A. Wolff, R.W. Malone, P. Williams, W. Chong, G. Acsadi, A. Jani, P.L. Felgner, Direct gene transfer into mouse muscle in vivo, Science (New York, N.Y.) 247 (1990) 1465–1468.
[15] S. Kreiter, A. Selmi, M. Diken, M. Koslowski, C.M. Britten, C. Huber, O. Tureci, U. Sahin, Intranodal vaccination with naked antigen-encoding RNA elicits potent prophylactic and therapeutic antitumoral immunity, Cancer Res. 70 (2010) 9031–9040.
[16] P. Midoux, C. Pichon, Lipid-based mRNA vaccine delivery systems, Expert Rev. Vaccines 14 (2015) 221234.
[17] K.K. Phua, S.K. Nair, K.W. Leong, Messenger RNA (mRNA) nanoparticle tumour vaccination, Nano 6 (2014) 7715–7729.
[18] M.P. Stewart, A. Sharei, X. Ding, G. Sahay, R. Langer, K.F. Jensen, In vitro and ex vivo strategies for intracellular delivery, Nature 538 (2016) 183–192.
[19] K. Broos, K. Van der Jeught, J. Puttemans, C. Goyvaerts, C. Heirman, H. Dewitte, R. Verbeke, I. Lentacker, K. Thielemans, K. Breckpot, Particle-mediated intravenous delivery of antigen mRNA results in strong antigen-specific T-cell responses despite the induction of type I interferon, Mol. Ther. Nucleic Acids 5 (2016) e326.
[20] B. Scheel, S. Braedel, J. Probst, J.P. Carralot, H. Wagner, H. Schild, G. Jung, H.G. Rammensee, S. Pascolo, Immunostimulating capacities of stabilized RNA molecules, Eur. J. Immunol. 34 (2004) 537–547.
[21] S.S. Diebold, C. Massacrier, S. Akira, C. Paturel, Y. Morel, C. Reis e Sousa, Nucleic acid agonists for Toll-like receptor 7 are defined by the presence of uridine ribonucleotides, Eur. J. Immunol. 36 (2006) 3256–3267.
[22] F. Heil, H. Hemmi, H. Hochrein, F. Ampenberger, C. Kirschning, S. Akira, G. Lipford, H. Wagner, S. Bauer, Species-specific recognition of single-stranded RNA via toll-like receptor 7 and 8, Science (New York, N.Y.) 303 (2004) 1526–1529.
[23] E. Brencicova, S.S. Diebold, Nucleic acids and endosomal pattern recognition: how to tell friend from foe? Front. Cell. Infect. Microbiol. 3 (2013) 37.
[24] L.M. Kranz, M. Diken, H. Haas, S. Kreiter, C. Loquai, K.C. Reuter, M. Meng, D. Fritz, F. Vascotto, H. Hefesha, C. Grunwitz, M. Vormehr, Y. Husemann, A. Selmi, A.N. Kuhn, J. Buck, E. Derhovanessian, R. Rae, S. Attig, J. Diekmann, R.A. Jabulowsky, S. Heesch, J. Hassel, P. Langguth, S. Grabbe, C. Huber, O. Tureci, U. Sahin, Systemic RNA delivery to dendritic cells exploits antiviral defence for cancer immunotherapy, Nature 534 (2016) 396–401.
[25] M.A. Oberli, A.M. Reichmuth, J.R. Dorkin, M.J. Mitchell, O.S. Fenton, A. Jaklenec, D.G. Anderson, R. Langer, D. Blankschtein, Lipid nanoparticle assisted mRNA delivery for potent cancer immunotherapy, Nano Lett. 17 (2017) 1326–1335.
[26] A. De Beuckelaer, J. Grooten, S. De Koker, Type I interferons modulate CD8 + T cell immunity to mRNA vaccines, Trends Mol. Med. 23 (2017) 216–226.
[27] A. De Beuckelaer, C. Pollard, S. Van Lint, K. Roose, L. Van Hoecke, T. Naessens, V.K. Udhayakumar, M. Smet, N. Sanders, S. Lienenklaus, X. Saelens, S. Weiss, G. Vanham, J. Grooten, S. De Koker, I. Type, Interferons interfere with the capacity of mRNA Lipoplex vaccines to elicit cytolytic T cell responses, Mol. Ther. 24 (2016) 2012–2020.
[28] C. Iavarone, T.D. O'Hagan, D. Yu, N.F. Delahaye, J.B. Ulmer, Mechanism of action of mRNA-based vaccines, Expert Rev. Vaccines 16 (2017) 871–881.
[29] T. Pepini, A.-M. Pulichino, T. Carsillo, A.L. Carlson, F. Sari-Sarraf, K. Ramsauer, J.C. Debasitis, G. Maruggi, G.R. Otten, A.J. Geall, D. Yu, J.B. Ulmer, C. Iavarone, Induction of an IFN-mediated antiviral response by a self-amplifying RNA vaccine: implications for vaccine design, J. Immunol. (2017).
[30] J. Devoldere, H. Dewitte, S.C. De Smedt, K. Remaut, Evading innate immunity in nonviral mRNA delivery: don't shoot the messenger, Drug Discov. Today (2015).
[31] O. Andries, M.D. Filette, S.C. De Smedt, J. Demeester, M.V. Poucke, L. Peelman, N.N. Sanders, Innate immune response and programmed cell death following carrier-mediated delivery of unmodified mRNA to respiratory cells, J. Control. Release 167 (2013) 157–166.
[32] B.R. Anderson, H. Muramatsu, B.K. Jha, R.H. Silverman, D. Weissman, K. Karikó, Nucleoside modifications in RNA limit activation of 2′-„5′-„oligoadenylate synthetase and increase resistance to cleavage by RNase L, Nucleic Acids Res. 39 (2011) 9329–9338.
[33] O. Andries, S. Mc Cafferty, S.C. De Smedt, R. Weiss, N.N. Sanders, T. Kitada, N(1)-methylpseudouridine-incorporated mRNA outperforms pseudouridine-incorporated mRNA by providing enhanced protein expression and reduced immunogenicity in mammalian cell lines and mice, J. Control. Release 217 (2015) 337–344.
[34] K. Kariko, M. Buckstein, H. Ni, D. Weissman, Suppression of RNA recognition by Toll-like receptors: the impact of nucleoside modification and the evolutionary origin of RNA, Immunity 23 (2005) 165–175.
[35] K. Kariko, H. Muramatsu, F.A. Welsh, J. Ludwig, H. Kato, S. Akira, D. Weissman, Incorporation of pseudouridine into mRNA yields superior nonimmunogenic vector with increased translational capacity and biological stability, Mol. Ther. 16 (2008) 1833–1840.
[36] M.S. Kormann, G. Hasenpusch, M.K. Aneja, G. Nica, A.W. Flemmer, S. Herber-Jonat, M. Huppmann, L.E. Mays, M. Illenyi, A. Schams, M. Griese, I. Bittmann, R. Handgretinger, D. Hartl, J. Rosenecker, C. Rudolph, Expression of therapeutic proteins after delivery of chemically modified mRNA in mice, Nat. Biotechnol. 29 (2011) 154–157.
[37] L.F. Fries, D.M. Gordon, R.L. Richards, J.E. Egan, M.R. Hollingdale, M. Gross, C. Silverman, C.R. Alving, Liposomal malaria vaccine in humans: a safe and potent adjuvant strategy, Proc. Natl. Acad. Sci. U. S. A. 89 (1992) 358–362.
[38] C.R. Alving, M. Rao, N.J. Steers, G.R. Matyas, A.V. Mayorov, Liposomes containing lipid A: an effective, safe, generic adjuvant system for synthetic vaccines, Expert Rev. Vaccines 11 (2012) 733–744.
[39] J. Neidhart, K.O. Allen, D.L. Barlow, M. Carpenter, D.R. Shaw, P.L. Triozzi, R.M. Conry, Immunization of colorectal cancer patients with recombinant baculovirus-derived KSA (Ep-CAM) formulated with monophosphoryl lipid A in liposomal emulsion, with and without granulocyte-macrophage colony-stimulating factor, Vaccine 22 (2004) 773–780.
[40] C.D. Platt, J.K. Ma, C. Chalouni, M. Ebersold, H. Bou-Reslan, R.A. Carano, I. Mellman, L. Delamarre, Mature dendritic cells use endocytic receptors to capture and present antigens, Proc. Natl. Acad. Sci. U. S. A. 107 (2010) 4287–4292.
[41] M. Diken, S. Kreiter, A. Selmi, C.M. Britten, C. Huber, O. Tureci, U. Sahin, Selective uptake of naked vaccine RNA by dendritic cells is driven by macropinocytosis and abrogated upon DC maturation, Gene Ther. 18 (2011) 702–708.
[42] H. Dewitte, R. Verbeke, K. Breckpot, R.E. Vandenbroucke, C. Libert, S.C. De Smedt, I. Lentacker, Choose your models wisely: how different murine bone marrow-derived dendritic cell protocols influence the success of nanoparticulate vaccines in vitro, J. Control. Release (2014).
[43] M.P. Monopoli, C. Aberg, A. Salvati, K.A. Dawson, Biomolecular coronas provide the biological identity of nanosized materials, Nat. Nanotechnol. 7 (2012) 779–786.
[44] G. Caracciolo, D. Pozzi, A.L. Capriotti, C. Cavaliere, S. Piovesana, G. La Barbera, A. Amici, A. Lagana, The liposome-protein corona in mice and humans and its implications for in vivo delivery, J. Mater. Chem. B 2 (2014) 7419–7428.
[45] D. Simberg, S. Weisman, Y. Talmon, A. Faerman, T. Shoshani, Y. Barenholz, The role of organ vascularization and lipoplex-serum initial contact in intravenous murine lipofection, J. Biol. Chem. 278 (2003) 39858–39865.

[46] S. Motta, V. Rondelli, L. Cantu, E. Del Favero, M. Aureli, D. Pozzi, G. Caracciolo, P. Brocca, What the cell surface does not see: the gene vector under the protein corona, Colloids Surf. B: Biointerfaces 141 (2016) 170–178.
[47] S. Even-Chen, R. Cohen, Y. Barenholz, Factors affecting DNA binding and stability of association to cationic liposomes, Chem. Phys. Lipids 165 (2012) 414–423.
[48] D. Hirsch-Lerner, M. Zhang, H. Eliyahu, M.E. Ferrari, C.J. Wheeler, Y. Barenholz, Effect of "helper lipid" on lipoplex electrostatics, Biochim. Biophys. Acta 1714 (2005) 71–84.
[49] S. Schöttler, G. Becker, S. Winzen, T. Steinbach, K. Mohr, K. Landfester, V. Mailänder, F.R. Wurm, Protein adsorption is required for stealth effect of poly (ethylene glycol)- and poly(phosphoester)-coated nanocarriers, Nat. Nanotechnol. 11 (2016) 372–377.
[50] J.S. Suk, Q. Xu, N. Kim, J. Hanes, L.M. Ensign, PEGylation as a strategy for improving nanoparticle-based drug and gene delivery, Adv. Drug Deliv. Rev. 99 ((2016) 28–51.
[51] B.R. Anderson, H. Muramatsu, S.R. Nallagatla, P.C. Bevilacqua, L.H. Sansing, D. Weissman, K. Karikó, Incorporation of pseudouridine into mRNA enhances translation by diminishing PKR activation, Nucleic Acids Res. 38 (2010) 5884–5892.
[52] Y. Kumagai, O. Takeuchi, H. Kato, H. Kumar, K. Matsui, E. Morii, K. Aozasa, T. Kawai, S. Akira, Alveolar macrophages are the primary interferon-alpha producer in pulmonary infection with RNA viruses, Immunity 27 (2007) 240–252.
[53] J.E. Pulverer, U. Rand, S. Lienenklaus, D. Kugel, N. Zietara, G. Kochs, R. Naumann, S. Weiss, P. Staeheli, H. Hauser, M. Koster, Temporal and spatial resolution of type I and III interferon responses in vivo, J. Virol. 84 (2010) 8626–8638.
[54] B.D. Brown, G. Sitia, A. Annoni, E. Hauben, L.S. Sergi, A. Zingale, M.G. Roncarolo, L.G. Guidotti, L. Naldini, In vivo administration of lentiviral vectors triggers a type I interferon response that restricts hepatocyte gene transfer and promotes vector clearance, Blood 109 (2007) 2797–2805.
[55] L. Pyfferoen, E. Brabants, C. Everaert, N. De Cabooter, K. Heyns, K. Deswarte, M. Vanheerswynghels, S. De Prijck, G. Waegemans, M. Dullaers, H. Hammad, O. De Wever, P. Mestdagh, J. Vandesompele, B.N. Lambrecht, K.Y. Vermaelen, The transcriptome of lung tumor-infiltrating dendritic cells reveals a tumor-supporting phenotype and a microRNA signature with negative impact on clinical outcome, Oncoimmunology 6 (2017).
[56] L.M. Wakim, J. Smith, I. Caminschi, M.H. Lahoud, J.A. Villadangos, Antibody-targeted vaccination to lung dendritic cells generates tissue-resident memory CD8 T cells that are highly protective against influenza virus infection, Mucosal Immunol. 8 (2015) 1060–1071.
[57] M.A. Willart, H. Jan de Heer, H. Hammad, T. Soullie, K. Deswarte, B.E. Clausen, L. Boon, H.C. Hoogsteden, B.N. Lambrecht, The lung vascular filter as a site of immune induction for T cell responses to large embolic antigen, J. Exp. Med. 206 (2009) 2823–2835.
[58] J.C. Kaczmarek, A.K. Patel, K.J. Kauffman, O.S. Fenton, M.J. Webber, M.W. Heartlein, F. DeRosa, D.G. Anderson, Polymer-lipid nanoparticles for systemic delivery of mRNA to the lungs, Angew. Chem. Int. Ed. Eng. 55 (2016) 13808–13812.
[59] N. Pardi, M.J. Hogan, R.S. Pelc, H. Muramatsu, H. Andersen, C.R. DeMaso, K.A. Dowd, L.L. Sutherland, R.M. Scearce, R. Parks, W. Wagner, A. Granados, J. Greenhouse, M. Walker, E. Willis, J.-S. Yu, C.E. McGee, G.D. Sempowski, B.L. Mui, Y.K. Tam, Y.-J. Huang, D. Vanlandingham, V.M. Holmes, H. Balachandran, S. Sahu, M. Lifton, S. Higgs, S.E. Hensley, T.D. Madden, M.J. Hope, K. Karikó, S. Santra, B.S. Graham, M.G. Lewis, T.C. Pierson, B.F. Haynes, D. Weissman, Zika virus protection by a single low-dose nucleoside-modified mRNA vaccination, Nature 543 (2017) 248–251.
[60] N. Pardi, S. Tuyishime, H. Muramatsu, K. Kariko, B.L. Mui, Y.K. Tam, T.D. Madden, M.J. Hope, D. Weissman, Expression kinetics of nucleoside-modified mRNA delivered in lipid nanoparticles to mice by various routes, J. Control. Release 217 (2015) 345–351.
[61] N. Pardi, A.J. Secreto, X. Shan, F. Debonera, J. Glover, Y. Yi, H. Muramatsu, H. Ni, B.L. Mui, Y.K. Tam, F. Shaheen, R.G. Collman, K. Kariko, G.A. Danet-Desnoyers, T.D. Madden, M.J. Hope, D. Weissman, Administration of nucleoside-modified mRNA encoding broadly neutralizing antibody protects humanized mice from HIV-1 challenge, Nat. Commun. 8 (2017) 14630.
[62] R.J. Dearman, M. Cumberbatch, G. Maxwell, D.A. Basketter, I. Kimber, Toll-like receptor ligand activation of murine bone marrow-derived dendritic cells, Immunology 126 (2009) 475–484.
[63] S. Van Lint, C. Goyvaerts, S. Maenhout, L. Goethals, A. Disy, D. Benteyn, J. Pen, A. Bonehill, C. Heirman, K. Breckpot, K. Thielemans, Preclinical evaluation of TriMix and antigen mRNA-based antitumor therapy, Cancer Res. 72 (2012) 1661–1671.
[64] S. Van Meirvenne, L. Straetman, C. Heirman, M. Dullaers, C. De Greef, V. Van Tendeloo, K. Thielemans, Efficient genetic modification of murine dendritic cells by electroporation with mRNA, Cancer Gene Ther. 9 (2002) 787–797.
[65] K. Braeckmans, K. Buyens, W. Bouquet, C. Vervaet, P. Joye, F. De Vos, L. Plawinski, L. Doeuvre, E. Angles-Cano, N.N. Sanders, J. Demeester, S.C. De Smedt, Sizing nanomatter in biological fluids by fluorescence single particle tracking, Nano Lett. 10 (2010) 4435–4442.